TITLE

Change in motor state equilibrium explains the prokinetic effect of apomorphine on locomotion in experimental Parkinsonism

Authors

Burce Kabaoglu[1], Elisa L. Garulli[1], Rafael De Sa[1], Arend Vogt[2], Ruben Behrsing[1], Matej Skrobot[3], Raik Paulat[1], Moritz Gerster[4,5,6], Wolf-Julian Neumann[7], Matthias Endres[1,8,9-11], Christoph Harms[1,8,9], Nikolaus Wenger[1]

Affiliations

[1] Department of Neurology with Experimental Neurology, Charité – Universitätsmedizin Berlin, Charitéplatz 1, 10117 Berlin, Germany

[2] Neuroscience Research Center (NWFZ), Charité – Universitätsmedizin Berlin, Charitéplatz 1, 10117 Berlin, Germany

[3] Berlin Institute of Health Julius Wolff Institut - Center for Musculoskeletal Biomechanics and Regeneration, Charité - Universitätsmedizin Berlin, Luisenstraße 65, 10115 Berlin, Germany

[4] Research Group Neural Interactions and Dynamics, Department of Neurology, Max Planck Institute for Human Cognitive and Brain Sciences, Leipzig, Germany

[5] Neurophysics Group, Department of Neurology, Charité – Universitätsmedizin Berlin

[6] Bernstein Center for Computational Neuroscience, Berlin, Germany

[7] Movement Disorders and Neuromodulation Section, Charité – Universitätsmedizin Berlin, Charitéplatz 1, 10117 Berlin, Germany

[8] Center for Stroke Research Berlin, Charité - Universitätsmedizin Berlin, Germany

[9] DZHK (German Center for Cardiovascular Research), Berlin Site, Germany

[10] DZNE (German Center for Neurodegenerative Disease), Berlin Site, Germany

[11] DZPG (German Center of Mental Health), Berlin Site, Germany

Correspondence to N.W. (nikolaus.wenger@charite.de), Dpt. of Neurology with Experimental Neurology, 10117 Berlin, Germany.

Short title

Motor state equilibrium explains prokinetic effect of apomorphine

---

Word count of the manuscript: 4676

Abstract

Gait impairments remain an unresolved challenge in Parkinson's disease (PD). Clinical studies highlight the importance of neural oscillations underlying motor deficits. Yet, how dopaminergic medication impacts brain activity for gait therapy remains poorly understood. To address this issue, we explored the influence of apomorphine on cortical oscillations during self-initiated locomotion on a runway in the unilateral 6-OHDA rat model of PD. In this task, deficits are characterized by slow movements and repeated interruptions of the gait sequence. Our results show that apomorphine reduced akinesia, increased voluntary transitions to gait, and prolonged individual gait bouts leading to an overall increase in the travel distance on the runway. In contrast, kinematic analysis revealed that these prokinetic changes were accompanied by a reduction in leg velocity and step length. At the neural level, behavioral changes correlated with a shift from beta and low-gamma to high-gamma brain rhythms. Beta and low-gamma significantly correlated with reduced transitions to gait, while high-gamma lead to a shift away from akinesia to prokinetic motor states. Together, our results provide new insights into the cortical regulation of locomotion and reveal the potential of apomorphine to differentially regulate gait sequence execution and gait kinematics. We propose that the prokinetic effects of apomorphine are best explained by the concept of a motor state equilibrium that is defined by the observable motor states, their durations and number of state transitions. This concept provides a simplified representation of complex treatment effects and holds promise to improve data interpretation for clinical translation.

Introduction

Parkinson's disease (PD) is a neurodegenerative disease characterized by the gradual death of dopaminergic neurons, which impact motor activities and cause symptoms such as tremors, bradykinesia, and gait impairments[1]. While dopaminergic medication and DBS may temporarily alleviate bradykinesia during gait, their efficacy diminishes over time, due to treatment fluctuations and disease progression[2–4]. Freezing of gait (FoG), a debilitating symptom of PD, is characterized by a sudden, transient inability to initiate or continue walking, often described by patients as feeling like their feet are "glued" to the floor[5,6]. The occurrence of FoG is often associated with disease severity and an increased risk of falls[7]. A better understanding of the underlying neural correlates of gait deficits may play a crucial role in defining new treatment strategies.

Excessive oscillatory neuronal activity in the beta frequency range (13-35 Hz) in the basal ganglia and motor cortex is a defining characteristic of Parkinson's disease in patients[1,8,9]. Such oscillatory activity is hypothesized to contribute to bradykinesia and rigidity[8], and is known to decrease following dopaminergic therapy and deep brain stimulation (DBS)[10]. Both therapies also increase gamma oscillations (65-90 Hz) that are generally considered to promote

movement in PD[9,11]. Additionally, Pogosyan et al. have shown that beta activity is a hallmark of sustaining a given motor state, i.e. promoting tonic contractions while suppressing the processing of new movements[12]. Based on these findings, Engel and Fries have proposed that beta oscillations signal the system's tendency to maintain the current motor state — in other words, to preserve the "status quo"[13]. In line with the "status quo" hypothesis, PD patients respond to "stop" cues more slowely when in the medication-off state and when beta oscillations are high[14]. However, patients also respond to "stop" cues more slowly during DBS ON states when beta oscillations are low[15], suggesting that the relationship between beta activity and motor control is complex and warrants further investigations.

Neural oscillations in PD have been predominantly studied for hand movements and motion artefacts have rendered perioperative neural recordings during locomotion difficult[16]. Recent clinical studies, using new device technologies, have provided first evidence that cortical oscillations may play an important role as a biomarker for gait deficits in PD. For example, the occurrence of FoG episodes has been associated with elevated low-beta oscillations in STN[17], the occurrence of low-frequency decoupling between motor cortex regions and the STN[7], and the increase of phase-amplitude coupling in the high beta-gamma range in motor cortex[18]. Yet, a better understanding how brain rhythms regulate locomotion during gait therapy is needed.

Rodent models of PD recapitulate many of the pathological neural oscillations and gait deficits observed in patients[4,19–22]. For example, neural correlates of rodent bradykinesia are found in the beta and low-gamma frequency range (approx. 15–40 Hz)[19], and their suppression is achieved with dopaminergic medication and deep brain stimulation[4,23]. Similar to the findings in PD patients, excessive activity in the high gamma range (HG, 70-110 Hz) coincides with the onset of dyskinesia in rats[24–26]. Cortical oscillations play an important role during walking in PD rodent models[4]. For example, in the unilateral 6-OHDA model during treadmill walking, beta and low-gamma oscillations are increased in comparions to sham, indicating abnormal motor cortical synchronization linked to gait[21]. Yet, the neural oscillations underlying gait execution in PD and their relationship to detailed kinematic activity warrant deeper exploration.

Here, we studied the self-initiated locomotion on a runway in the unilateral 6-OHDA rat model using high-resolution video cameras synchronized with 3D hindlimb kinematics and motor cortex ECOG recordings. From the video analysis we identified three principal motor states during gait task execution: namely gait, akinesia, and exploratory movements without forward locomotion (here referred to as stationary movements). To alleviate locomotor deficits, we used therapeutic dosages of apomorphine that promoted forward locomotion without inducing extensive unilateral rotations. Our results showed that apomorphine increased the overall travel distance on the runway by reducing time spent in akinesia, increasing voluntary transitions to gait, and prolonging individual gait bouts. In contrast, apomorphine decreased stepping velocity and step length measured from hindlimb kinematics. These combined

behavioral changes correlated with a shift from beta and low-gamma oscillations to high-gamma. Apomorphine induced changes on brain rhythms were selectively observed during episodes of stationary movement and gait, but not during time periods of akinesia. Additionally, the correlations of neural oscillations with state transitions indicated that beta and low-gamma specifically reduce voluntary transitions to gait, and high-gamma promoted transitions away from akinesia to prokinetic activity. Together, we propose that these complex behavioral observations are best explained by the concept of a motor state equilibrium, defined by observable motor states, their durations and number of transitions. Within this framework, the treatment effect of apomorphine can be represented as a shift in motor state equilibrium and the role of neural oscillations can be interpreted as a function of each ongoing motor state. The insights from this study may help the future refinement of clinical data analysis and improve ongoing developments of closed-loop neuromodulation strategies for gait therapy in PD.

Methods

Ethics statement

All experimental procedures were approved by the local regulatory bodies (Federal Office for Health and Social Affairs, Berlin, Germany; approval number: G0206/19) and performed in compliance with the German Animal Welfare Act. The experimental procedures were performed on male Sprague-Dawley rats (n = 26, 300–325 g, Janvier, France). Animals were kept on a 12-hour light cycle with ad libitum access to food and water. The data of this study can be made available by the corresponding author upon request.

Surgical Procedures and Lesioning

Unilateral lesioning of midbrain dopaminergic neurons was performed on 8-week-old rats to model Parkinson's disease. During the surgery, anesthesia was maintained with 1-1.5% isoflurane in oxygen. The body temperature was regulated with a heating mat, and the breathing rate was monitored with an oximeter (MouseOx). Upon anesthesia induction, rats received a subcutaneous injection of carprofen (5 mg/kg) for pain management. They were then secured in a stereotactic frame (David Kopf Instruments, Tujunga, CA). Local anesthesia was provided under the scalp with 2% lidocaine (B. Braun SE, Germany), and corneal dehydration was prevented with Pan-Ophtal Gel eye ointment. The surgical site was prepared by excising skin to fully expose the skull. The dorsoventral distance between bregma and lambda was adjusted to less than 0.05 mm for accurate targeting. Using the Paxinos coordinate system, the skull was marked and a craniotomy was performed. We used a 33-gauge blunt steel needle to deliver 1 µL of solution containing 0.05% ascorbic acid and 8 µg of 6-OHDA (Sigma-Aldrich, Taufkirchen, Germany) in 0.9% sterile saline. The injection was performed into the left medial forebrain bundle (MFB) at specified coordinates (AP: −2.6, ML: +1.6, DV: −8.4, DV measured from the skull surface) using a precision pump (Harvard

Apparatus, Massachusetts, MA, USA). The needle was left in place at the target site for 5 minutes following the infusion of the neurotoxin.

Electrocorticography (ECoG) electrode implantations with 1.2 mm stainless steel scre electrodes were performed 2 weeks after the initial lesion. The preparation and protective measures were identical with the first surgery with added steps for electrode implantation and head stage installation. The frontal, parietal, and interparietal bones were carfully cleared from connective tissue, rinsed with sterile saline, and dried with an air blower. The exposed skull surface was then treated with a UV-activated bonding agent (OptiBond All-in-One, Kerr). A surgical pen was used to mark the sites of the craniotomies. Another UV-activated dental composite, Charisma (Kulzer, Germany), was then put on top of the OptiBond layer to make a shallow well. The subsequent craniotomy and durotomy allowed for the stereotactic implantation of a custom-made stainless-steel screw (1,2mm of diameter) overlaying motor cortex (AP: +3.75, ML: ±2; Ground, AP: −12.5, ML: −2) The electrodes were attached with silver wires to a 32-channel connector (polarized nano connector, PZN, Omnetics). The electronic components were subsequently encapsulated in dental acrylic (Paladur, Kulzer, Germany). After the surgery, we allowed the animals to recover for three days under close observation and administration of daily pain medication (carprofen, 5 mg/kg s.c.).

Apomorphine dosages

Apomorphine (Sigma-Aldrich, Taufkirchen, Germany) was administered s.c. at 0.025 mg/kg for gait therapy in the runway experiments. For the induction of body rotations in the cyclinder test at the end of experiments we used an apomorphine dosage of 0.05 mg/kg. For both tasks, the specified amount of apomorphine was applied approx. 5 min before the start of the experiments.

Behavioral Data Acquisition

Runway experiments

Rats were handled daily starting approx. two weeks prior to 6-OHDA lesioning (experimental timeline see Fig 1A). The animals were then trained for three days on the runway to habituate themselves to the experimental environment. For all runway trials in this study, we placed a home cage with a second rat at the end of the runway. This allowed for a quick habituation of the animals and sufficient motivation to repeatedly engage in the runway task. For each run, rats were placed by an experimenter at the beginning of the runway. After a fixed time of 2 min the trial was terminated by picking up the animal at its final position, shuttling it to the homecage and after approx. 3-5 seconds shuttling it back again to the start of the runway. Hindlimb kinematics were captured using a high-speed motion capture system (Vicon), which included 12 infrared cameras and two high definition video cameras, operating at a recording frequency of 200 Hz and 40 Hz, respectively[27]. Reflective markers were attached to key anatomical

landmarks on both hindlimbs (iliac crest, hip, knee, ankle, front quadrant of the foot) and the shoulders (Fig 2). Kinematic parameters were analyzed and computed using custom-written MATLAB scripts[27].

Runway experiments started one week after ECOG implantation, corresponding to three weeks after 6-OHDA lesioning. In the same session, rats were recorded OFF medication and after application of a therapeutic dose of apomorphine (s.c. at 0.025 mg/kg). For each condition, rats were allowed to traverse the runway until data were collected from 15 trials. Each trial began with the animal being placed at one beginning of the runway. A trial was considered successful and terminated, if the animal traversed the runway continuously to the end of the runway. If the animal paused or failed to initiate walking, the trial was stopped after two minutes. Trials continued until 10 successful runs were completed or until 15 minutes had elapsed. During data analysis, videos were manually annotated to define the beginning and end of the motor states of akinesia, stationary movement, and gait in the software Nexus 2.0 (Vicon).

Cylinder Test

One week after electrode implantation, the effectiveness of the 6-OHDA lesion was assessed behaviorally using an apomorphine challenge within a glass cylinder. Behavior in the cylinder was documented using a video camera (ELP 1080P, Night Vision USB Camera, 30Hz framerate). Following baseline recordings of 5 min OFF medication, we administered a dose of apomorphine at 0,05mg/kg. Five minutes after injection, the rats were returned to the glass cylinder; Rotation trajectories were reconstructed using the DeepLabCut software package[28]. We quantified and analyzed the rotations ipsilateral and contralateral to the dopaminergic lesion using custom-written MATLAB script.

Neural Data Acquisition

Neural data were acquired using a multicomponent system from Tucker-Davis Technologies (RZ2, TDT, Alachua, FL, USA). The system was set to enable neural recordings at 6 kHz. Recording cables were connected to the freely behaving animals through a motorized commutator (ACO32, TDT). Neural signals were digitized locally at the head of the animal with a 32 channel digitizing headstage (Intan).

Power and Frequency

Power spectral densities of M1 electrocorticograms (ECoGs) were computed using fast Fourier transform (FFT) with a Hanning window and a frequency resolution of 1 Hz. The resulting power spectra were subsequently decomposed into aperiodic and oscillatory components employing the FOOOF toolbox[29]. The FOOOF algorithm (version 1.1.0) and default settings were used for the algorithm (i.e., no custom parameter adjustments). Power spectra were parameterized across the frequency range 5 to 120 Hz. We defined specific frequency ranges

for analysis: the beta and low-gamma range spanned from 25 to 45 Hz, and the high-gamma range spanned 70 to 100 Hz. The power analysis within these bands was expressed in arbitrary units (a.u.) without additional normalization.

Histology

The extent of dopaminergic denervation was assessed post-mortem through immunohistological staining for tyrosine hydroxylase (TH). Under deep anesthesia, animals were transcardially perfused with 70 mL of 0.1 M phosphate-buffered saline containing 0.4% sodium-heparin, followed by 120 mL of 4% w/v paraformaldehyde in 0.1 M phosphate buffer. Subsequently, brains were extracted, postfixed in 4% w/v paraformaldehyde for a minimum of 24 hours, and cryoprotected sequentially in 15% and 30% sucrose solutions for 24 hours and one week, respectively. Tissues were then frozen in methylbutane (Carl Roth, Karlsruhe, Germany).

40-µm coronal cryo-sections encompassing the entire striatum from −3.24 to 2.52 relative to bregma were serially cut. Sections underwent a 30-minute preincubation in quenching solution (100 mM glycine, pH 7.4, adjusted with 2M Tris Base), followed by a 30-minute incubation in blocking solution. They were then incubated overnight at 4°C with rabbit anti-rat tyrosine hydroxylase antibody (Abcam, Cambridge, UK) and anti-NeuN (neuron nucleus) antibody (Merck Millipore, CA) diluted in blocking solution. After three 10-minute washes in PBS, the sections were incubated for 2 hours at room temperature with secondary antibodies: anti-rabbit-594 (#A-21207, Invitrogen, Eugene, OR, USA) and anti-mouse-488 (#A-11029, Invitrogen, Eugene, OR, USA), along with DAPI (1:10000) in blocking solution. Finally, the sections were rinsed with PBS and mounted with ImmuMount. The stained slices were imaged using a Leica DMI8 microscope, allowing detailed visualization of the stained dopaminergic neurons and nuclei.

The optical density (OD) of TH+ fibers in the striatum was measured using NIH ImageJ (version 2.9.0). OD values were calculated by subtracting the background signal (measured in the unstained corpus callosum) from both the lesioned and unlesioned striatal measurements. Three striatal sections per animal were analyzed.

Statistics

Video raters were blinded to group allocations to minimize bias. Statistical quantification of individual outcome parameters was performed using a nonparametric, two-way factorial design (Scheirer-Ray-Hare Test) for the factors drug condition and motor state. Post-hoc analysis was conducted with the Wilcoxon signed rank test for within-group comparisons and the Mann-Whitney U test for between-group comparisons. All p-values are of exploratory nature.

Results

Neural correlates of global locomotor deficits in the 6-OHDA model on the runway

We first assessed the effect of apomorphine on travel distance and average traversal speed, two global motor deficits on the runway in the unilateral 6-OHDA lesion rat model. Average traversal speed was defined as the travel distance divided by each trial's duration. The timeline of experimental procedures is shown in Figure 1A. We confirmed the successfull induction of the PD model post mortem with TH stainings, which showed a prominent reduction (>95%) of TH innervation in the striatum of the lesioned hemisphere (Fig. 1B). During behavioral experiments, rats were placed on an elevated runway (Fig. 2A). Therapeutic dosages of apomorphine (0.025 mg/kg) were administered to modulate network activity and promote straight walking. Results showed that PD rats traveled shorter distances in the medication-OFF condition compared to apomorphine, 60 cm (± 15.20 SD) versus 80 cm (± 13.33 SD), respectively (Fig. 2B). In contrast, there was no detectable change in the average traversal speed following apomorphine administration.

We then correlated these features to the changes in cortical oscillations following apomorphine administration. Medication-OFF recordings showed a pronounced peak in the beta and low-gamma range (25-45 Hz) (Fig. 2C). Apomorphine reduced the power of this frequency range with a large effect size (1.48 ± 0.54 SD; 1.15 ± 0.41 SD; Cohen's d=0.66) but did not reach statistical significance for group comparisons. High gamma was significantly increased after apomorphine treatment (0.66 ± 0.21 SD; 0.83 ± 0.19 SD; p=0.003). Correlations of travel distance with the beta and low-gamma range did not show signficance Spearman r = -0.32, p = 0.093). Instead, high-gamma significantly correlated with travel distance (Spearman r = 0.5, p = 0.007). The average traversal speed did not correlate with either of the two assessed frequency ranges (Spearman r = -0.11, p = 0.57; r = 0.31, p = 0.11) (Fig. 2D). In summary, travel distance was selectively correlated with cortical high gamma activity.

Apomorphine prolongs time spent in gait while reducing akinesia

In a next step, we expanded our analysis to distinguish between the three main motor states observed in the gait task: namely gait, akinesia and stationary movements. High-resolution video recordings were manually annotated to mark the start and end of each motor state (Supplementary video 1).

During each runway trial, PD rats in medication-OFF conditions spent roughly 4.68 seconds (± 2.77 SD) in gait, which increased to 11.74 seconds (± 5.43 SD) after apomorphine injection. The time spent in stationary movement decreased from 26.39 (± 10.15 SD) seconds to 14.63 (± 10.21 SD) seconds and for akinesia from 11.59 (± 6.53 SD) seconds to 2.41 (± 4.51 SD) seconds. All changes were statistically significant (Fig. 3A).

We then analysed cortical oscillations selectively during each motor state (Fig. 3C). Beta and low-gamma power significantly decreased for comparisons between akinesia and the other two prokinetic states (Supplementary Fig. 2). However, apomorphine administration had no significant effect on beta and low-gamma during akinetic episodes (Fig. 2c). High gamma changes showed a similar picture, with no significant effect of apomorphine during akinesia, but with a selective increase in power during stationary movements and gait (Fig. 2C and Supplementary Fig. 2).

Neurobehavioral relationships further showed three significant correlations between cortical oscillations and the duration of selective motor states (Fig. 3D). First, beta and low-gamma power were negatively (Spearman $r = -0.53$, $p = 0.0037$), and high-gamma positively correlated (Spearman $r = 0.49$, $p = 0.0086$) with gait duration. High-gamma negatively correlated with stationary movement duration (Spearman $r = -0.39$, $p = 0.042$). Together, these results point towards a distinct role of cortical oscillations in regulating durations of specific motor states.

Apomorphine reduces stepping velocity and step during self-inititated gait

Using our 3D kinematic recordings, we further explored selective changes of gait cycle features in the hindlimbs. As previously reported, we calculated a set of 104 kinematic parameters[30] and subjected them to principal component analysis (PCA) (Fig. 4B). Gait patterns were visualized in PC1 and PC2 space, where PC1 explained the most variance (26%) and significantly distinguished the med-ON and OFF conditions (Fig. 4B). Factor analysis revealed that therapeutic dosages of apomorphine led to slower and smaller steps during gait episodes (Fig. 4B, right panel). The most correlated factor loadings on PC1 included gait velocity, step length, and double stance duration (Fig. 4C).

Correlating beta and low-gamma with the PC1 score showed no significant relationship (Spearman $r = 0.22$, $p = 0.26$). Instead, elevation in high-gamma significantly correlated with the kinematic changes (Spearman $r = -0.39$, $p = 0.038$) (Fig. 4E). Together, apomorphine prolonged gait episodes, but these longer episodes were associated with slower hindlimb movement.

Apomorphine alters motor state transitions during self-initiated locomotion

To further delineate how apomorphine acts on the execution of the gait sequence, we calculated the transitions between each motor state (Fig. 5A). Apomorphine significantly reduced the number of all observed motor state transitions (medication OFF: 5.60 ± 2.15. SD; apomorphine: 3.68 ± 1.38 SD; $p = 0.004$) and the transitions between stationary movement and akinesia (medication-OFF: 28.57 ± 8.49 SD; apomorphine: 6.75 ± 9.85. SD; $p = 0.0002$) (Fig 5B). In contrast, the number of transitions between stationary movement and gait was

increased (medication-OFF: 2.21 ± 0.87. SD; apomorphine: 3.01 ± 0.95 SD; $p = 0.02$). In our experiments, we did not observe any direct transitions between gait and akinesia.

Correlating neural oscillations with the state transitions showed that the beta and low-gamma power negatively correlated with the number of stationary movement to gait transitions (Spearman $r = -0.40$, $p = 0.036$). High gamma negatively correlated with the number of transitions between stationary movement and akinesia (Spearman $r = -0.45$, $p = 0.015$) (Fig. 5C). In summary, these results show that cortical high-gamma helps to drive the system away from akinesia into prokinetic states, while the reduction of beta and low-gamma are significantly implicated in enabling voluntary transitions to gait.

Discussion

This study examined neurobehavioral alterations in locomotion at baseline and after apomorphine administration in a rat model of Parkinson's disease. Apomorphine demonstrated prokinetic effects in the Parkinson's disease rat model. The intervention specifically reduced the power of HB-LG oscillations while increasing the power of HG oscillations, resulting in extended gait episodes. Furthermore, increased HG oscillations correlated with a decrease in the duration of stationary movement and an impaired gait pattern, while maintaining the duration of the gait state. Apomorphine reduced the frequency of transitions between motor states and increased the proportion of transitions from stationary movement to gait. Together, these complex results point towards a selective role of cortical oscillations for each motor state and their transitions during locomotion.

Oscillatory mechanisms of motor state regulation: a dynamic equilibrium model in Parkinson's disease

Evidence from PD patients provides support for the status quo hypothesis, which suggests that beta oscillations help maintain the current motor state. In the akinetic OFF state (without dopaminergic treatment), cortical–basal ganglia coherence is dominated by beta-band activity[9]. Following levodopa administration (ON state), beta activity is reduced, and a peak emerges in the gamma band. Similarly, during movement preparation and execution, beta activity decreases in the OFF state, while gamma coherence increases in the ON state[31].

Our findings align with this framework but offer a new interpretation. We propose a model in which the durations of, and transitions between, motor states in Parkinson's disease exist in a dynamic equilibrium, as illustrated in Figure 6. Under baseline PD conditions, this equilibrium favors frequent transitions between akinesia and stationary movement, supported by pronounced HB-LG and reduced HG oscillations — maintaining the "status quo" of idleness. Apomorphine decreases HB-LG power and amplifies HG power, thereby extending the duration of and maintaining the gait episodes. Contrary to the established observation that beta activity decreases during motion execution[13], we find that reduced HB-LG activity leads to fewer transitions between stationary movement and gait, effectively stabilizing the gait state.

Furthermore, increased HB-LG activity combined with reduced low HG activity correlates with shorter gait episodes at baseline, suggesting that it is the balance between these oscillations—rather than HB-LG activity alone—that functions as an idling mechanism.

Moreover, heightened HG activity reduces transitions between stationary movement and akinesia, effectively eliminating akinesia episodes. Our results show that HG activity correlates negatively with the duration of stationary movement and the number of transitions between stationary movement and akinesia, while correlating positively with gait duration. This supports the hypothesis that gamma oscillations have prokinetic properties. However, we refine this interpretation: the heightened bradykinetic gait characteristics observed under increased HG activity suggest that labeling HG purely as “prokinetic” is somewhat misleading, as it does not restore a healthy gait pattern. Instead, HG oscillations promote the maintenance of motor states by reducing transitions between them and are specifically anti-akinetic by suppressing transitions into the akinetic state.

Taken together, these results suggest that motor state regulation and gait kinematics are governed by distinct locomotor networks, with HG and HB-LG oscillations playing differential roles in modulating state transitions.

Gait Kinematics

While beta and gamma oscillations modulate transitions between motor states, our findings suggest that these rhythms are less involved in modulating gait kinematics. In particular, we found no significant relationship between HB-LG power and gait parameters, indicating that cortical beta activity may not be a reliable marker or an effective target for modifying movement execution. This observation aligns with Jiang et al. 2024, who reported that neither beta nor gamma power correlated with movement velocity in lesioned rats[19]. Additionally, although gamma power is often associated with prokinetic effects, its correlation with bradykinetic gait in our study suggests a more nuanced role. Rather than directly influencing kinematics, gamma oscillations may serve to stabilize ongoing motor states, including gait, by reducing transitions into akinesia. This distinction is crucial: whereas pathological oscillations may contribute to gait freezing or instability, their modulation does not necessarily translate into improvements in gait quality. Therefore, while oscillatory activity in the motor cortex provides insight into state regulation, the control of gait kinematics may be governed by parallel or downstream motor circuits that are less directly reflected in M1 ECoG signals. Understanding this dissociation is essential for refining therapeutic strategies aimed at improving gait in PD, and highlights the need for complementary approaches targeting spinal or subcortical locomotor networks.

Two potential mechanisms may account for the worsened gait features observed in the apomorphine condition. Dopamine has been shown to modulate spinal circuits[32]. Koblinger et al. demonstrated that optogenetic activation of dopaminergic neurons in the diencephalic A11 region, which projects to the spinal cord, can initiate locomotion[33]. The exacerbated

pathological gait observed in the PD apomorphine condition may result from apomorphine's direct effects on dopamine receptors within the spinal cord.

Secondly, Skovgard et al. have shown that L-DOPA, the D1 agonist SKF82958, and the D2 agonist sumanirole all induce pronounced narrow band gamma (NBG) (70-110 Hz) oscillations in the rostral forelimb area (RFA), which coincide with dyskinesia[26]. Arber and Costa describe corticospinal projections from the RFA into cervical spinal cord domains[34]. The axon terminals of these projections align with premotor neurons in the spinal cord, which then project into extensor and flexor premotor neurons. These findings collectively suggest that the exacerbated bradykinetic gait observed in our study may stem from apomorphine-induced activity changes in the motor cortex, which subsequently affect spinal premotor circuits, thereby offering a thorough understanding of the neural mechanisms underlying locomotion deficits.

Limitations

This study offers a comprehensive analysis of locomotor behavior, separate from gait kinematics; however, several potential limitations must be acknowledged. Firstly, there is a lack of neural data during akinesia episodes in the apomorphine condition, as these episodes were absent in 9 out of 14 animals. This absence makes it challenging to comment on the representation of akinesia in the motor cortex. Secondly, the behavioral experiments were conducted under illuminated conditions to ensure optimal video recording quality. The elevated runway utilized in this study is comparable to the open arm of an elevated plus maze, a conventional apparatus for assessing anxiety-related behaviors in rodents[35]. Despite habituating the animals to the experimental room for five days, the combination of bright lights and the elevated, open platform may have induced anxiety-like freezing behaviors. This is especially pertinent considering the established correlation between anxiety and freezing of gait in patients[36]. Future experiments could employ a non-elevated runway and night vision cameras to separate the effects of anxiety from the observed changes in motor behavior in this study.

Acknowledgments

N.W., C.H., and M.E. conceived and designed the study. B.K. performed the lesion surgeries and electrode implantations. B.K. and E.L.G. acquired data. B.K., E.L.G., and M.G. analyzed data. R.D.S., A.V., R.B., M.S., and R.P. provided technical support. N.W., C.H., and M.E. secured funding and resources. N.W. supervised the project. B.K. and N.W. wrote the manuscript. All authors read and approved the final version of the manuscript.

Sources of funding

E.L.G., B.K., W.J.N., M.E., C.H., and N.W. received support from the Collaborative Research Center ReTune (TRR 295, project number 424778381). W.J.N. was additionally funded by the European Research Council (ERC, ReinforceBG, project 101077060) and the German Federal Ministry of Education and Research (BMBF, project FKZ01GQ1802). M.E. received further support from the German Research Foundation (DFG) under Germany's Excellence Strategy (EXC-2049 – 390688087) and the Clinical Research Group KFO 5023 BeCAUSE-Y (project 2, EN343/16-1), as well as from the BMBF, DZNE, DZHK, DZPG, the EU, the Corona Foundation, and Fondation Leducq. C.H. was funded by the DFG (Excellence Strategy, EXC-2049 – 390688087, SPARK-BIH Stroke Protect), the EraNet Neuron project (DFG project 522473931), the DZHK/BMBF Innovation Cluster (FKZ81X2100285), Charité 3R (C3RHeaD and STROKE-PREDICT-C3R), the BIH, and the Fondation Leducq Transatlantic Network of Excellence (17CVD03).

Conflict of interest

WJN received honoraria for consulting from InBrain – Neuroelectronics that is a neurotechnology499company and honoraria for talks from Medtronic that is a manufacturer of deep brain stimulation500devices unrelated to this manuscript.

Citations

Declaration of generative AI and AI-assisted technologies in the writing process

During the preparation of this work the author(s) used OpenAI / ChatGPT-4o in order to improve language and readability. After using this tool/service, the author(s) reviewed and edited the content as needed and take(s) full responsibility for the content of the publication.

1. Moustafa AA, Chakravarthy S, Phillips JR, Gupta A, Keri S, Polner B, Frank MJ, Jahanshahi M. Motor symptoms in Parkinson's disease: A unified framework. *Neuroscience & Biobehavioral Reviews*. 2016;68:727–740.

2. Mirelman A, Bonato P, Camicioli R, Ellis TD, Giladi N, Hamilton JL, Hass CJ, Hausdorff JM, Pelosin E, Almeida QJ. Gait impairments in Parkinson's disease. *Lancet Neurol*. 2019;18:697–708.

3. Pötter-Nerger M, Volkmann J. Deep brain stimulation for gait and postural symptoms in Parkinson's disease. *Mov Disord*. 2013;28:1609–1615.

4. Wenger N, Vogt A, Skrobot M, Garulli EL, Kabaoglu B, Salchow-Hömmen C, Schauer T, Kroneberg D, Schuhmann MK, Ip CW, et al. Rodent models for gait network disorders in Parkinson's disease – a translational perspective. *Experimental Neurology*. 2022;352:114011.

5. Hardeman LES, Kal EC, Young WR, van der Kamp J, Ellmers TJ. Visuomotor control of walking in Parkinson's disease: Exploring possible links between conscious movement processing and freezing of gait. *Behavioural Brain Research*. 2020;395:112837.

6. Nutt JG, Bloem BR, Giladi N, Hallett M, Horak FB, Nieuwboer A. Freezing of gait: moving forward on a mysterious clinical phenomenon. *Lancet Neurol*. 2011;10:734–744.

7. Pozzi NG, Canessa A, Palmisano C, Brumberg J, Steigerwald F, Reich MM, Minafra B, Pacchetti C, Pezzoli G, Volkmann J, et al. Freezing of gait in Parkinson's disease reflects a sudden derangement of locomotor network dynamics. *Brain*. 2019;142:2037–2050.

8. Kühn AA, Kupsch A, Schneider G-H, Brown P. Reduction in subthalamic 8-35 Hz oscillatory activity correlates with clinical improvement in Parkinson's disease. *Eur J Neurosci*. 2006;23:1956–1960.

9. Brown P, Oliviero A, Mazzone P, Insola A, Tonali P, Di Lazzaro V. Dopamine dependency of oscillations between subthalamic nucleus and pallidum in Parkinson's disease. *J Neurosci*. 2001;21:1033–1038.

10. Mathiopoulou V, Lofredi R, Feldmann LK, Habets J, Darcy N, Neumann W-J, Faust K, Schneider G-H, Kühn AA. Modulation of subthalamic beta oscillations by movement, dopamine, and deep brain stimulation in Parkinson's disease. *npj Parkinson's Disease*. 2024;10:77.

11. Muthuraman M, Bange M, Koirala N, Ciolac D, Pintea B, Glaser M, Tinkhauser G, Brown P, Deuschl G, Groppa S. Cross-frequency coupling between gamma oscillations and deep brain stimulation frequency in Parkinson's disease. *Brain*. 2020;143:3393–3407.

12. Pogosyan A, Gaynor LD, Eusebio A, Brown P. Boosting cortical activity at Beta-band frequencies slows movement in humans. *Curr Biol*. 2009;19:1637–1641.

13. Engel AK, Fries P. Beta-band oscillations--signalling the status quo? *Curr Opin Neurobiol*. 2010;20:156–165.

14. Wylie SA, van Wouwe NC, Godfrey SG, Bissett PG, Logan GD, Kanoff KE, Claassen DO, Neimat JS, van den Wildenberg WPM. Dopaminergic medication shifts the balance between going and stopping in Parkinson's disease. *Neuropsychologia*. 2018;109:262–269.

15. Lofredi R, Auernig GC, Irmen F, Nieweler J, Neumann W-J, Horn A, Schneider G-H, Kühn AA. Subthalamic stimulation impairs stopping of ongoing movements. *Brain*. 2021;144:44–52.

16. Hell F, Plate A, Mehrkens JH, Bötzel K. Subthalamic oscillatory activity and connectivity during gait in Parkinson's disease. *NeuroImage: Clinical*. 2018;19:396–405.

17. Thenaisie Y, Lee K, Moerman C, Scafa S, Gálvez A, Pirondini E, Burri M, Ravier J, Puiatti A, Accolla E, et al. Principles of gait encoding in the subthalamic nucleus of people with Parkinson's disease. *Sci. Transl. Med.* 2022;14:eabo1800.

18. Yin Z, Zhu G, Liu Y, Zhao B, Liu D, Bai Y, Zhang Q, Shi L, Feng T, Yang A, et al. Cortical phase-amplitude coupling is key to the occurrence and treatment of freezing of gait. *Brain*. 2022;145:2407–2421.

19. Jiang X, Yang J, Wang Z, Jia J, Wang G. Functional interaction of abnormal beta and gamma oscillations on bradykinesia in parkinsonian rats. *Brain Res Bull*. 2024;209:110911.

20. Dupre KB, Cruz AV, McCoy AJ, Delaville C, Gerber CM, Eyring KW, Walters JR. Effects of L-dopa priming on cortical high beta and high gamma oscillatory activity in a rodent model of Parkinson's disease. *Neurobiol Dis*. 2016;86:1–15.

21. Brazhnik E, Novikov N, McCoy AJ, Ilieva NM, Ghraib MW, Walters JR. Early decreases in cortical mid-gamma peaks coincide with the onset of motor deficits and precede exaggerated beta build-up in rat models for Parkinson's disease. *Neurobiology of Disease*. 2021;155:105393.

22. Lemaire N, Hernandez LF, Hu D, Kubota Y, Howe MW, Graybiel AM. Effects of dopamine depletion on LFP oscillations in striatum are task- and learning-dependent and selectively reversed by ¡span class="smallcaps smallerCapital"¿l¡/span¿-DOPA. *Proceedings of the National Academy of Sciences*. 2012;109:18126–18131.

23. Li Q, Ke Y, Chan DCW, Qian Z-M, Yung KKL, Ko H, Arbuthnott GW, Yung W-H. Therapeutic deep brain stimulation in Parkinsonian rats directly influences motor cortex. *Neuron*. 2012;76:1030–1041.

24. Delaville C, McCoy AJ, Gerber CM, Cruz AV, Walters JR. Subthalamic Nucleus Activity in the Awake Hemiparkinsonian Rat: Relationships with Motor and Cognitive Networks. *J. Neurosci.* 2015;35:6918–6930.

25. Güttler C, Altschüler J, Tanev K, Böckmann S, Haumesser JK, Nikulin VV, Kühn AA, Riesen C van. Levodopa-Induced Dyskinesia Are Mediated by Cortical Gamma Oscillations in Experimental Parkinsonism. *Movement Disorders*. 2021;36:927–937.

26. Skovgård K, Barrientos SA, Petersson P, Halje P, Cenci MA. Distinctive Effects of D1 and D2 Receptor Agonists on Cortico-Basal Ganglia Oscillations in a Rodent Model of L-DOPA-Induced Dyskinesia. *Neurotherapeutics*. 2023;20:304–324.

27. van den Brand R, Heutschi J, Barraud Q, DiGiovanna J, Bartholdi K, Huerlimann M, Friedli L, Vollenweider I, Moraud EM, Duis S, et al. Restoring voluntary control of locomotion after paralyzing spinal cord injury. *Science*. 2012;336:1182–1185.

28. Mathis A, Mamidanna P, Cury KM, Abe T, Murthy VN, Mathis MW, Bethge M. DeepLabCut: markerless pose estimation of user-defined body parts with deep learning. *Nat Neurosci*. 2018;21:1281–1289.

29. Donoghue T, Haller M, Peterson EJ, Varma P, Sebastian P, Gao R, Noto T, Lara AH, Wallis JD, Knight RT, et al. Parameterizing neural power spectra into periodic and aperiodic components. *Nature Neuroscience*. 2020;23:1655–1665.

30. Wenger N, Moraud EM, Raspopovic S, Bonizzato M, DiGiovanna J, Musienko P, Morari M, Micera S, Courtine G. Closed-loop neuromodulation of spinal sensorimotor circuits

controls refined locomotion after complete spinal cord injury. *Science Translational Medicine*. 2014;6:255ra133.

31. Cassidy M, Mazzone P, Oliviero A, Insola A, Tonali P, Di Lazzaro V, Brown P. Movement-related changes in synchronization in the human basal ganglia. *Brain*. 2002;125:1235–1246.

32. Sharples SA, Koblinger K, Humphreys JM, Whelan PJ. Dopamine: a parallel pathway for the modulation of spinal locomotor networks. *Front Neural Circuits*. 2014;8:55.

33. Koblinger K, Jean-Xavier C, Sharma S, Füzesi T, Young L, Eaton SEA, Kwok CHT, Bains JS, Whelan PJ. Optogenetic Activation of A11 Region Increases Motor Activity. *Frontiers in Neural Circuits* [Internet]. 2018;12. Available from: https://www.frontiersin.org/articles/10.3389/fncir.2018.00086

34. Arber S, Costa RM. Networking brainstem and basal ganglia circuits for movement. *Nature Reviews Neuroscience*. 2022;23:342–360.

35. Walf AA, Frye CA. The use of the elevated plus maze as an assay of anxiety-related behavior in rodents. *Nature Protocols*. 2007;2:322–328.

36. Martens KAE, Hall JM, Gilat M, Georgiades MJ, Walton CC, Lewis SJG. Anxiety is associated with freezing of gait and attentional set-shifting in Parkinson's disease: A new perspective for early intervention. *Gait Posture*. 2016;49:431–436.

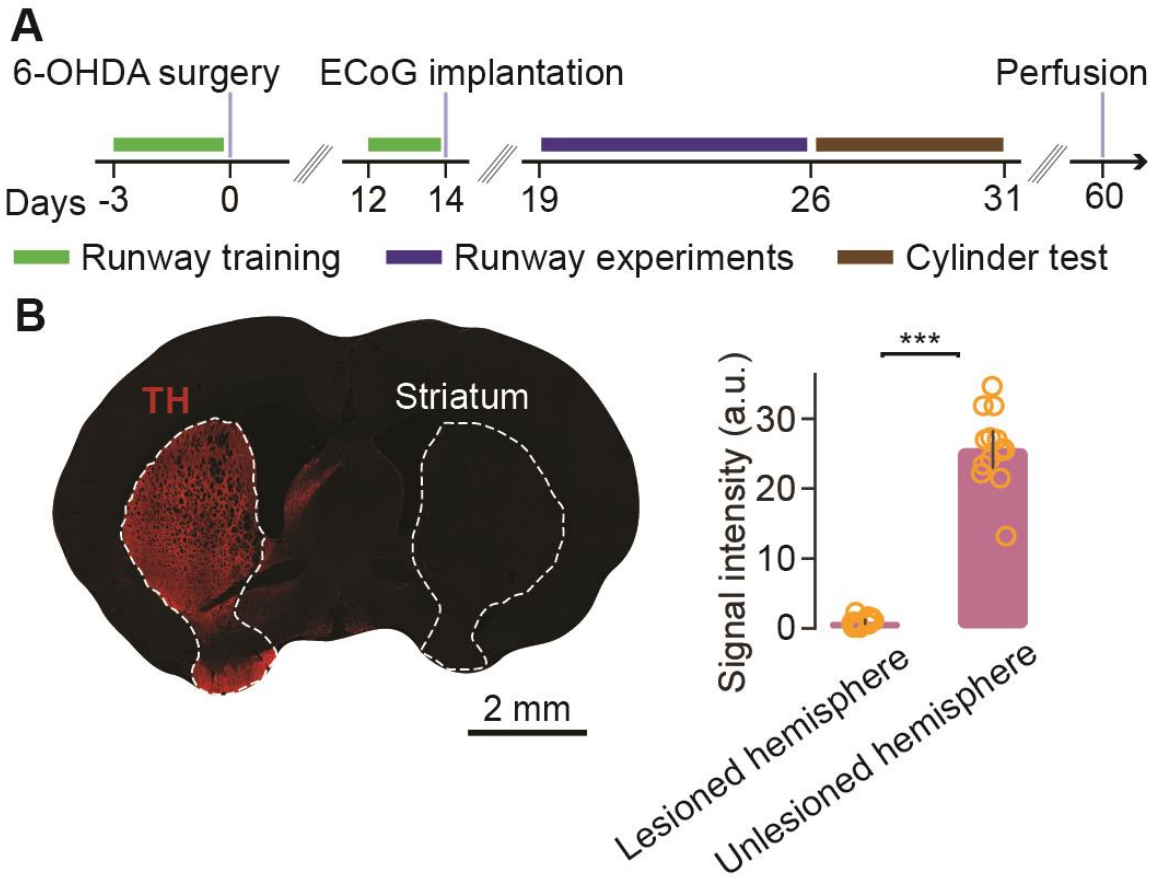

Figure 1. The experimental setup. (**A**) The timeline of interventions and experiments is depcited. The animals were habituated to the elevated runway starting 3 days before the 6-OHDA lesion surgery (green bar). They recoverd for 12 days and habituated to the runway for 2 days before the implantation surgery (green bar). Days before the 6-OHDA lesion are noted with a '-'. ECoG screws and LFP electrodes were implanted on day 14. The runway experiments of the baseline and apomorphine (0.025 mg/kg) took place between day 19 and day 26 (blue bar). Although the runway experiments spanned 7 days, each animal was tested on only one day within this period, with the specific testing day varying among animals. The 6-OHDA lesion was assessed by analyzing rotations induced by a high-dose of apomorphine (0.05 mg / kg) in a glass cylinder between days 26-31 (brown bar). After completing the behavioral experiments, the animals were used for another study, followed by transcardial perfusion and tissue collection on day 60. (**B**) Histological verification of the unilateral 6-OHDA lesion. Left: Representative coronal section labeled with an anti-tyrosine hydroxylase (TH) antibody. Red indicates the TH signal. White dashed line encircles the striatum. Right: Quantification of the TH signal intensity in the lesioned and unlesioned hemispheres of the TH labeled coronal sections (n=14 rats). Bars are reported as mean ± SD, *** $p<0.001$.

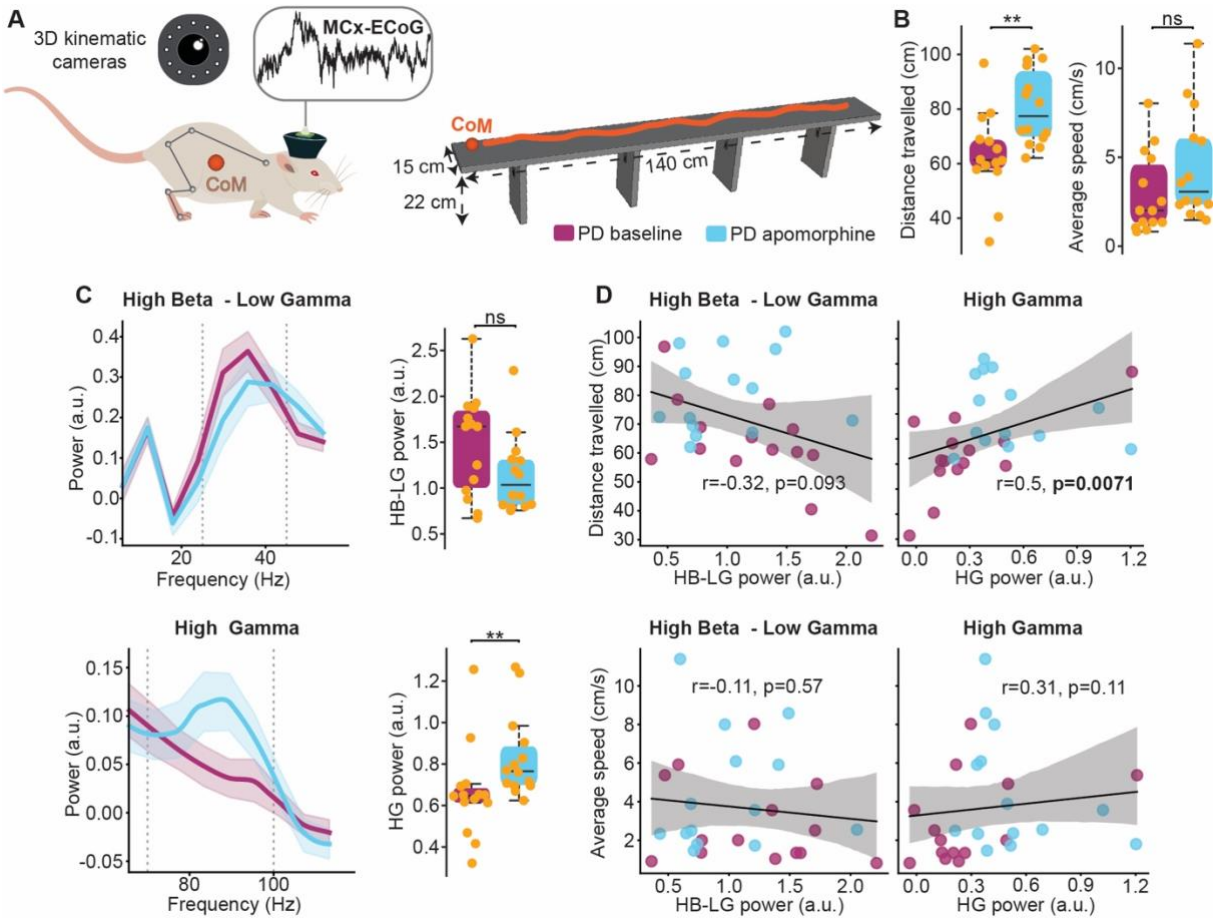

Figure 2. Apomorphine's action on spontenaeous locomotion on the runway. (**A**) Experimental setup for 3D-kinematic analysis based on infrared markers on the animal's body and synchronized neural recordings. Left: Neural and behavioral data collection elements. Gray spheres on the rat indicate the placement of the infrared markers. Center of mass is calculated as the gravity point of all labeled koints and indicated with 'CoM' in dark orange. Right: The elevated runway and its dimensions. The dark orange line represents the motion of the CoM over the runway. (**B)** The quantification of the distance travelled and the average whole-body speed on the runway. (**C**) Left: PSD plots for the HB-LG (top) and HG (bottom) frequency ranges. Power is shown in arbitrary units (a.u.). Gray dashed lines indicate 25 Hz and 45 Hz in the HB-LG plot, and 70 Hz and 100 Hz in the HG plot. Right: Quantification of the HB-LG and HG activity between the frequency range indicated as area under the curve. (**D**)The correlation of the HB-LG and HG power with the distance travelled and average traversal speed. Magenta represents the baseline and blue represents the apomorphine condition. Individual data points are represented with light orange dots. Boxplots show medians, 25% and 75% quartiles.Significance levels: ns $p>0.05$, ** $p<0.01$.

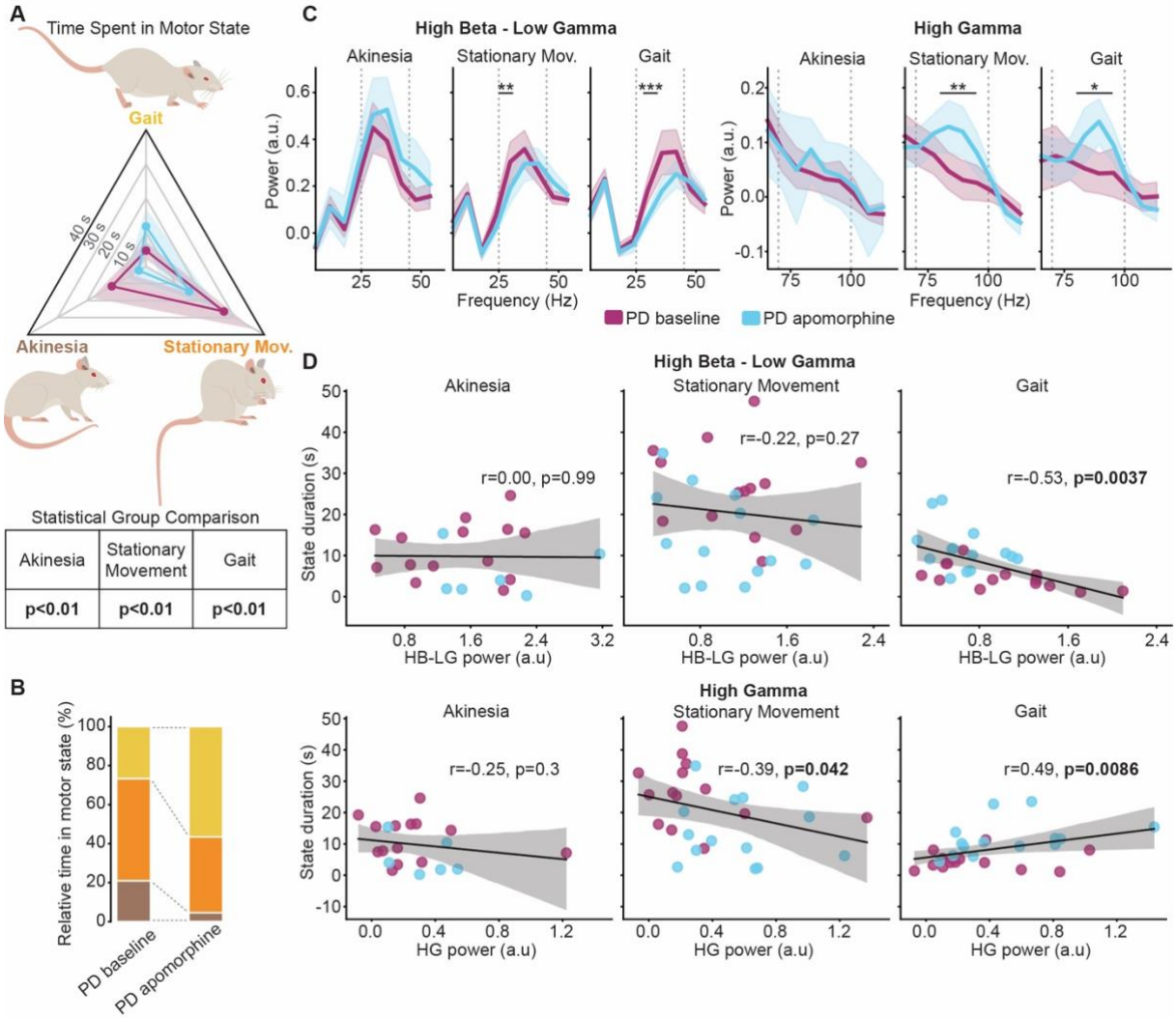

Figure 3. Behavioral and neural anaylsis for each individual motor state. (**A**) Top: Spider plot showing the average time (seconds) spent in the motor states of akinesia, stationary movement, and gait. Bottom: Statistical group comparison of the average state durations, with p-values obtained from the Wilcoxon signed-rank test.(**B**) Average proportions (%) of the motor states in PD baseline and PD apomorphine conditions. Brown represents akinesia, orange represents stationary movement, and yellow represents gait.(**C**) PSD plots for the HB-LG (left) and HG (right) frequency ranges across the three motor states. Power is shown in arbitrary units (a.u.). Gray dashed lines indicate 25 Hz and 45 Hz in the HB-LG plot, and 70 Hz and 100 Hz in the HG plot. Asterisks mark frequency ranges with significant differences in oscillatory activity between conditions: HB-LG stationary movement (25-33 Hz), HB-LG gait (29-37 Hz), HG stationary movement (80-95 Hz), and HG gait (80-95 Hz).(**D**) Correlation of HB-LG and HG power in motor states with the average duration of each motor state. Magenta represents the baseline, and blue represents the apomorphine condition. Significance levels: *p < 0.05, **p < 0.01, ***p < 0.001.

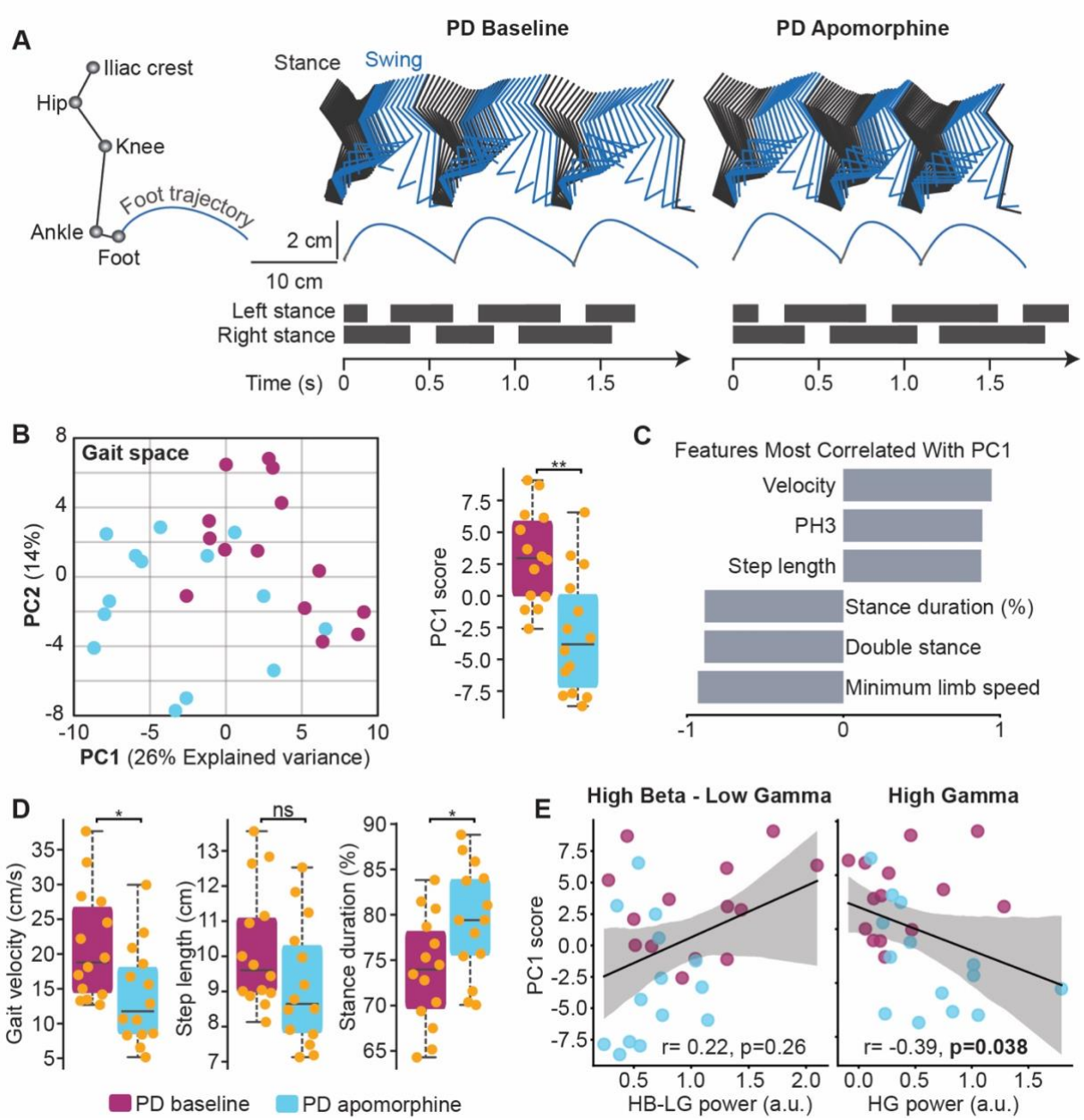

Figure 4. Influence of apomorphine on gait kinematics. (**A**) Left: Graphical illustration of the 'stick figure' representation of the hindlimb and foot trajectory. Right: (Top) Color-coded stick figure illustration of hindlimb movement during three consecutive steps, showing respective foot trajectories in baseline and apomorphine conditions. (Bottom) Stance durations illustrated with dark gray bars. (**B**) Left: Principal Component (PC) analysis for dimensionality reduction of 104 gait features. Right: PC1 scores for baseline and apomorphine conditions. (**C**) Gait features most correlated with the PC1 score. PH3: Phase of the elevation angle of the knee-ankle joint at maximal amplitude. Gait analysis revealed significant gait deterioration in the apomorphine condition, characterized by hindlimb bradykinesia. (**D**) Quantification of three representative gait features. (**E**) Correlation of HB-LG and HG power during the gait state with PC1 scores. Magenta represents the baseline, and blue represents the apomorphine

condition. Individual data points are represented with light orange dots. Boxplots show medians, 25% and 75% quartiles. Significance levels: ns $p > 0.05$, *$p < 0.05$, **$p < 0.01$.

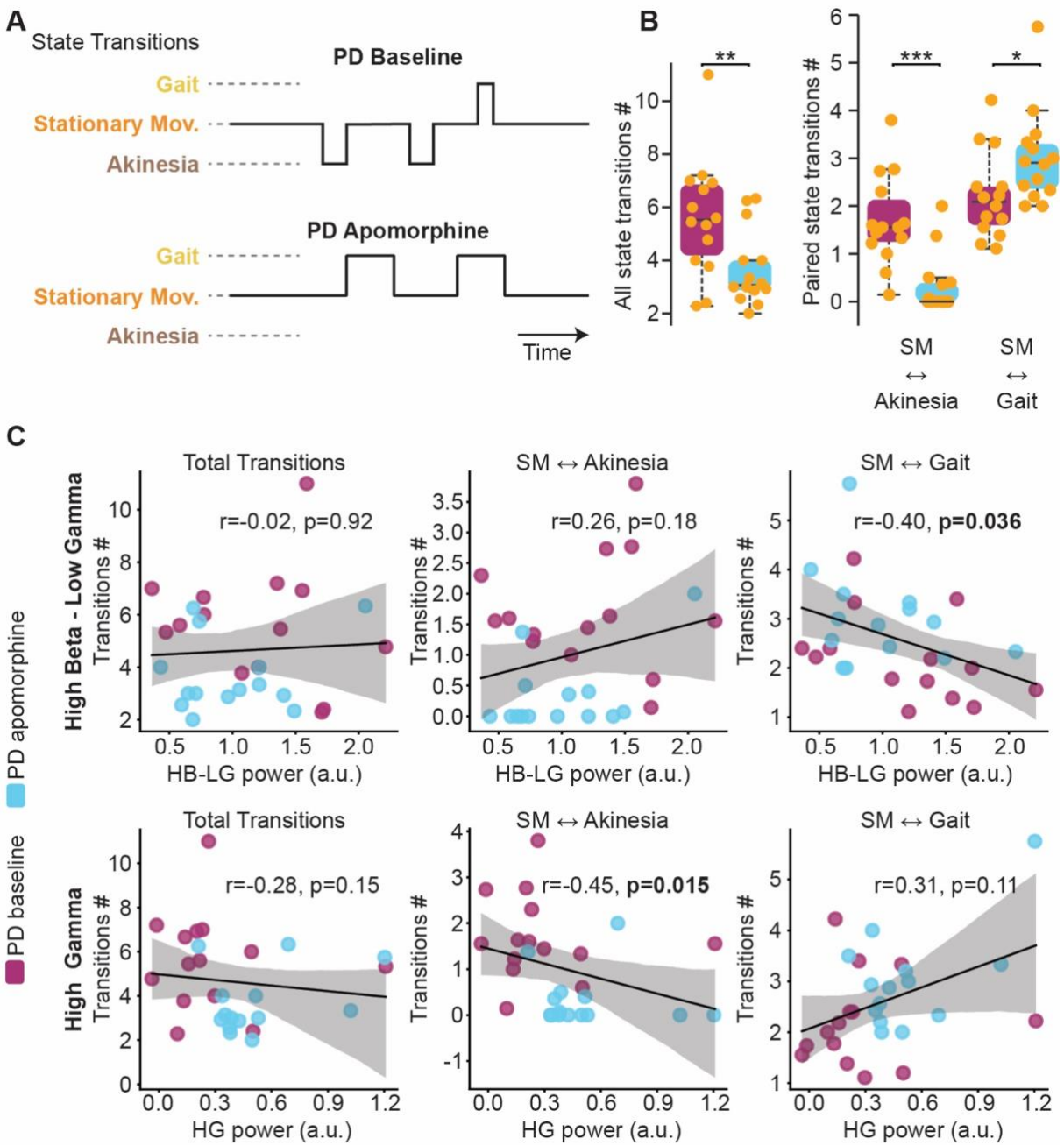

Figure 5. Analysis of motor state transitions (**A**) Graphical illustration of representative locomotor sequences in the baseline and apomorphine conditions. (**B**) Left: Quantification of net state transitions. Right: Transitions between akinesia ↔ stationary movement (SM) and gait ↔ stationary movement in baseline and apomorphine conditions. (**C**) Correlation of the number of transitions with total HB-LG and HG power. Magenta represents the baseline, and blue represents the apomorphine condition. Individual data points are represented with light orange dots. Boxplots show medians, 25% and 75% quartiles. Significance levels: *p < 0.05, **p < 0.01, ***p < 0.001.

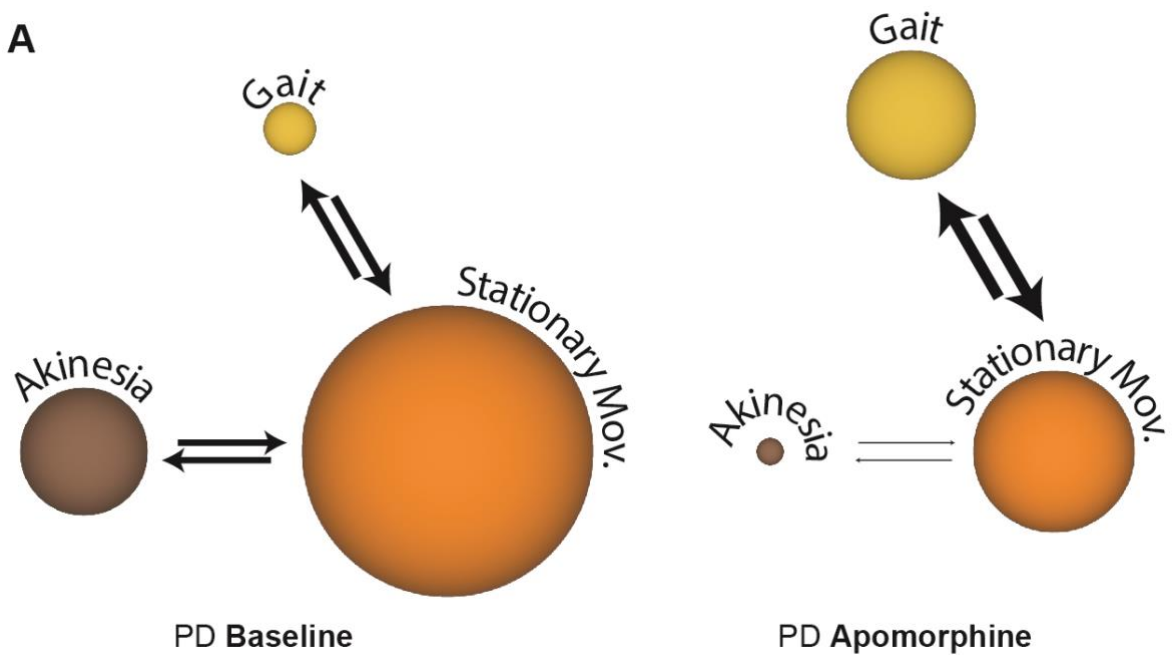

Figure 6. The motor state equilibrium.(**A**) Graphical representation of the proposed motor state equilibrium. The size of the spheres represents the average state duration, and arrow size indicates the average amount of state transitions per runway trial (PD: akinesia ↔ stationary movement=1.69, gait ↔ stationary movement=2.20; PD + apomoprhine: akinesia ↔ stationary movement=0.33, gait ↔ stationary movement =3.01). The equilibrium representations help to simplify the complex changes of low-dose apomorphine on spontaneous locomotion on the runway.

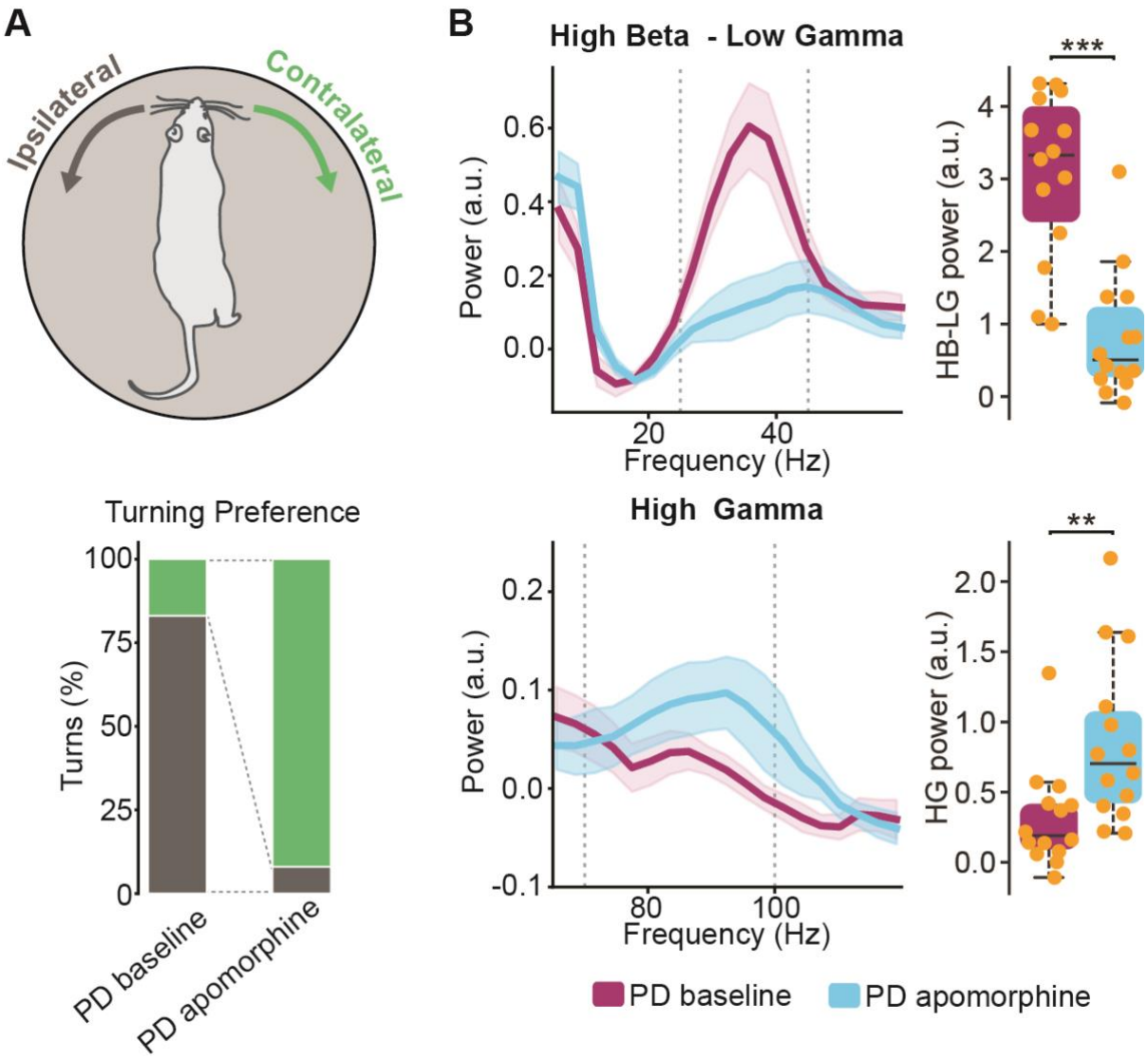

Supplementary Figure 1. The cylinder test.(**A**)Top: Graphical illustration of a rat inside the glass cylinder. Gray arrow represents turn to the ipsilateral side with the 6-OHDA lesion, green arrow represents turns to the contralateral side with the 6-OHDA lesion. Bottom: Average prooption of turns to the ipsilateral and contralateral side under the two conditions. (**B**) Left: PSD plots for the HB-LG (top) and HG (bottom) frequency ranges of the 5-minute recordings under the given condittion. Power is shown in arbitrary units (a.u.). Gray dashed lines indicate 25 Hz and 45 Hz in the HB-LG plot, and 70 Hz and 100 Hz in the HG plot. Right: Quantification of the HB-LG and HG activity between the frequency range indicated as area under the curve. Magenta represents the baseline and blue represents the apomorphine condition. Individual data points are represented with light orange dots. Boxplots show medians, 25% and 75% quartiles. Significance levels: ** $p<0.01$, *** $p<0.001$.

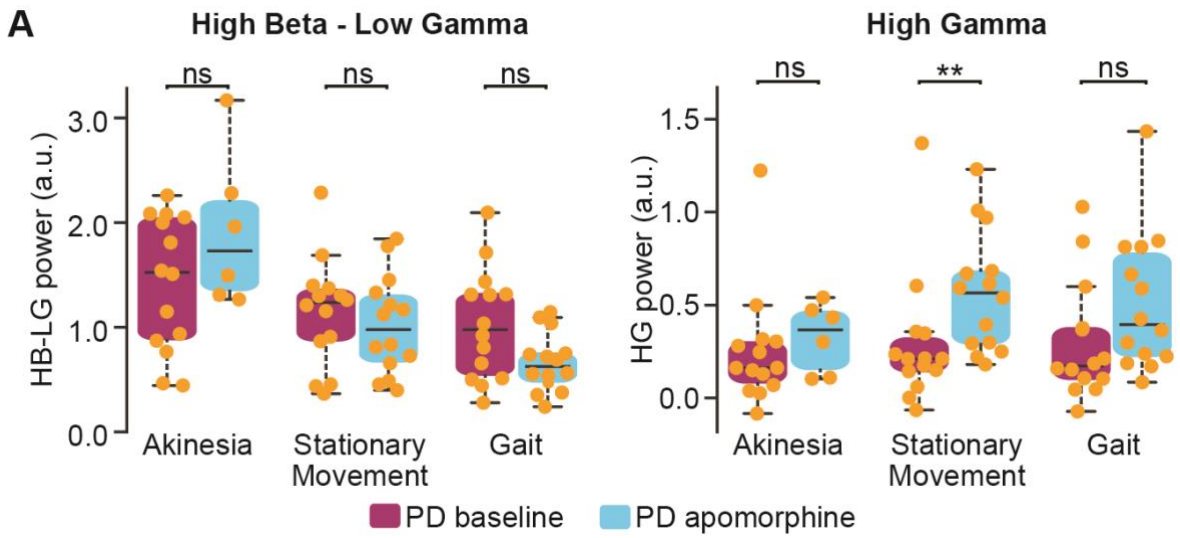

Supplementary Figure 2. Quantification of cortical activity during motor states.(**A**) Quantification of the HB-LG and HG activity in motor states (shown in **Fig.3C**) between the frequency range indicated as area under the curve. Individual data points are represented with light orange dots. Magenta represents the baseline and blue represents the apomorphine condition. Boxplots show medians, 25% and 75% quartiles. Significance levels: ns $p>0.05$, ** $p<0.01$.